

## Self-Organized Criticality in Fragmenting

Lene Oddershede,<sup>1,2</sup> Peter Dimon,<sup>3</sup> and Jakob Bohr<sup>1,\*</sup>

<sup>1</sup>*Department of Solid State Physics, Risø National Laboratory, DK-4000 Roskilde, Denmark*

<sup>2</sup>*Department of Physics, Odense University, DK-5230 Odense M, Denmark*

<sup>3</sup>*Niels Bohr Institute, University of Copenhagen, DK-2100 Copenhagen Ø, Denmark*

(Received 16 February 1993; revised manuscript received 3 September 1993)

The measured mass distributions of fragments from 26 fractured objects of gypsum, soap, stearic paraffin, and potato show evidence of obeying scaling laws; this suggests the possibility of self-organized criticality in fragmenting. The probability of finding a fragment scales inversely to a power of the mass; the power, or scaling exponent, was found to depend on the shape of the object rather than on the material. For objects of different shapes (balls, cubes, half cubes, plates, and bars) scaling was found for fragment sizes smaller than the smallest dimension of the object undergoing fragmentation.

PACS numbers: 46.30.Nz, 05.90.+m, 91.30.-f

The notion of self-organized criticality was put forward as a general principle for the late state evolution of dynamic systems: Correlations will appear on all length scales, and the system is critical. Global features will not depend on the microscopic mechanisms [1–3]. One of the first phenomena to be discussed in this context was 1/f noise [1]. The Gutenberg-Richter [4] scaling law for earthquakes has been interpreted as an example of self-organized criticality [5–8]. Computer simulations [1–3, 9–13] have addressed the concept of self-organized criticality, most notably that part describing the intrinsic behavior of sandpiles in which avalanches were found to appear on all length scales. Experiments carried out on the sandpile configuration have been inconclusive, and it has been suggested that the critical state emerges only for finite systems [14,15]. The propagation pattern for cracks has been shown to be fractal [16,17] and the growth of such cracks to be multifractal [18,19]. One way to understand this is to assume preexisting microfractures with the necessary properties [20]. Another model for fragmentation is based on partitioning of larger pieces into smaller ones. It shows that under certain conditions (a particular value of a tuning parameter) scaling should be present [21]. The appearance of a fractal size distribution of crushed ice has been discussed [22], and the fragmentation of long thin glass rods is shown to follow a log-normal distribution, which can be understood on the basis of a one-dimensional probability model [23,24]. The experimental distribution of fragments from glass spheres is a classic example of scaling [25].

In this paper we report on the observation of power law distributions of fragments from objects of gypsum. Objects of different shapes were cast of gypsum by pouring liquid gypsum into an open mold of the desired shape, thereby minimizing stresses and strains in the objects. In particular none of the objects was machined. After drying at room temperature for about a week the objects were fragmented by throwing them onto a hard floor, or in the case of especially solid bodies by striking them with a hammer. To prevent pieces from escaping, the frag-

mentation took place in the center of a large plastic sheet covering the floor. The mass of each fragment larger than  $10^{-2}$  g was measured by an electronic scale, and for those smaller (down to  $10^{-3}$  g) with an analytical balance. This procedure extended by one decade the range of masses considered, and it also verified that all fragments larger than  $10^{-2}$  g had indeed been collected using the electronic scale. The number of fragments measured varied from about 100 to 1000 depending on the size of the object.

The question that we address is whether the distribution  $n(m)$  describing the probability for finding a fragment of mass  $m$  exhibits scaling; i.e., does there exist a power  $\beta$  such that for an arbitrary length scale  $a$ ,

$$n(am) = a^{-\beta} n(m).$$

As measurements of the fracture distribution yield single events instead of the continuous probability distribution  $n(m)$ , it is more convenient to work with the total number of fragments with masses larger than or equal to  $m$ :  $\int_m^\infty n(m') dm'$ . If  $n(m)$  exhibits scaling with the exponent  $\beta$ , then for the integral the exponent is one larger. We therefore divide the integral by  $m$  such that it will show the same scaling exponent as  $n(m)$ :

$$N(m) = \frac{1}{m} \int_m^\infty n(m') dm'.$$

Figure 1 shows a double logarithmic plot of  $N(m)$  for a single experiment in which an approximately spherical gypsum ball of diameter 70 mm was fragmented. The data follow a power law for almost the entire range of masses; the exponent  $\beta$  is 1.63. Another gypsum ball of diameter 120 mm gave approximately the same value for  $\beta$ , 1.60; for a cube 74 mm on edge  $\beta$  was 1.56. Within the accuracy of the determination ( $\pm 0.05$ ) these numbers are consistent. It has been predicted theoretically and verified in experiments [25] that the exponent for the accumulated fragment distribution for a spherical glass ball is  $-\frac{2}{3}$ . In our notation this corresponds to a  $\beta$  of 1.67, a number not far from that observed.

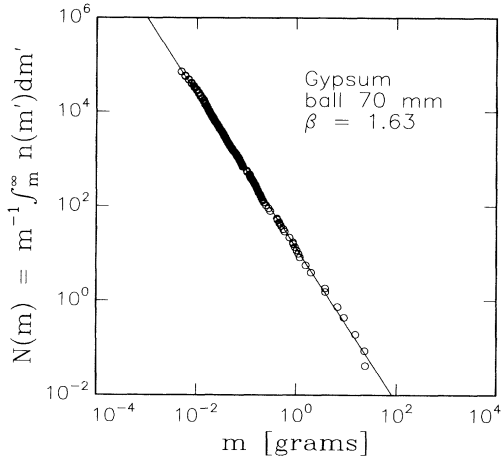


FIG. 1. The fragment distribution  $N(m)$  obtained from the fragmenting of a single spherical gypsum ball of diameter 70 mm. Over 4 decades of mass values, the data obey a scaling law leading to a rectilinear distribution on the double logarithmic plot. A least-squares fit to a line gives the estimate 1.63 for the exponent  $\beta$ .

Figure 2 shows  $N(m)$  for an experiment with a gypsum disk 320 mm in diameter and 5 mm thick. Scaling is present for smaller masses; for larger masses there is a tendency toward a more rapid decrease in the value of  $N(m)$ . We interpret this as a finite size cutoff, but note that it may also be described within the framework of a multifractal distribution [26]. The solid line in Fig. 2 is a fit by

$$N(m) = cm^{-\beta} \exp(-m/m_0),$$

where  $m_0$  is a characteristic finite size cutoff mass and  $c$  a scale factor. In the scaling region (small masses) in Fig. 2,  $\beta$  has a value of 1.08, which is significantly different from the exponent of the solid ball ( $\sim 1.63$ ). As the slopes of the disk and the ball differ, it follows that the change for  $m > m_0$  cannot be a dimensional crossover. Also in Fig. 2 the slope continues to decrease (to below  $-1.65$ ) for larger masses. The characteristic cutoff mass  $m_0$  for the fit in Fig. 2 is 0.51 g, corresponding to a volume of  $9 \times 9 \times 9$  mm<sup>3</sup>. This means that the scaling takes place only for fragments about the size and smaller than the thickness of the disk. Therefore, the scaling is essentially a three-dimensional phenomenon despite the two-dimensional nature of the disk on larger length scales.

Figure 3 shows the fragment distribution obtained for a bar of gypsum 1080 × 12 × 4 mm<sup>3</sup>. The fitted values of  $\beta$  and  $m_0$  are 1.05 and 0.19 g, the latter corresponding to a volume of  $6 \times 6 \times 6$  mm<sup>3</sup>. Scaling is present for fragments of size smaller than the smallest dimension of the bar.

In order to check for the dependence of the power on the way in which the object was fragmented, identical objects were struck in different ways. No evidence on such

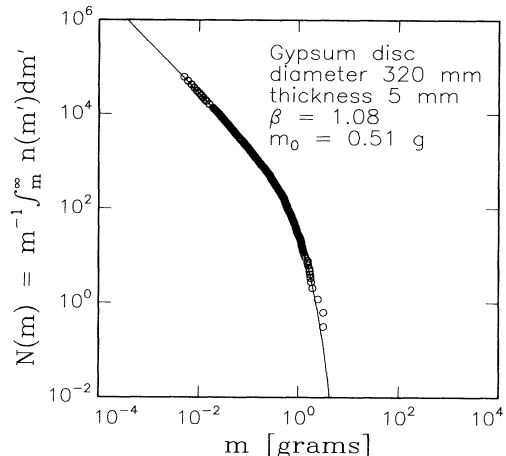


FIG. 2. The fragment distribution  $N(m)$  for a gypsum disk, 320 mm in diameter and 5 mm thick. Below a characteristic mass  $m_0$  approximately 0.51 g, scaling is obeyed and the exponent is 1.08. For masses above  $m_0$  the distribution falls off more rapidly; we have attributed this to finite size cutoff.

a dependence was seen. For example, three experiments with identical plates of dimensions  $195 \times 151 \times 4$  mm<sup>3</sup> were carried out. One was thrown horizontally onto the floor while the other two were thrown vertically down. The results of these three experiments can be seen in Table I. The power  $\beta$  is also given, and within the uncertainties they are equal. For the three identical plates mentioned above, the masses of the original objects  $M_0$  are listed in Table I; the variation of  $M_0$  is caused by differences in the thickness of the plates. The sum of the masses of pieces larger than  $10^{-2}$  g is called  $M_A$  and is given in Table I. The mass of the measured pieces smaller than  $10^{-2}$  g added together with the mass of the

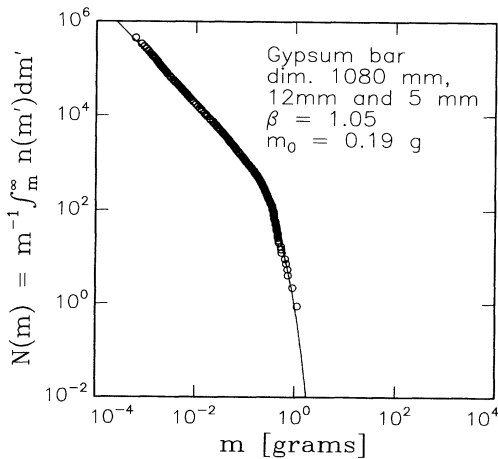


FIG. 3. The fragment distribution  $N(m)$  for a bar, dimension  $1080 \times 12 \times 4$  mm<sup>3</sup>. Below the characteristic mass 0.19 g scaling is obeyed and the corresponding exponent is 1.05.

TABLE I. Data from three experiments carried out with identical objects of dimensions  $195 \times 151 \times 4 \text{ mm}^3$ . One was thrown onto the floor horizontally, two vertically.  $M_0$  is the mass of the object before fragmentation.  $M_A$  is the total mass of the measured pieces larger than  $10^{-2} \text{ g}$ .  $M_B$  gives the value of the mass of the measured pieces smaller than  $10^{-2} \text{ g}$  added to the mass of the remaining dust and pieces.  $M_{\text{scaling}}$  is the integrated mass of the scaling distribution from  $10^{-2} \text{ g}$  to 0 g.  $\beta$  is the observed scaling exponent.

	$M_0 \text{ (g)}$	$M_A = \sum m_i, m_i \geq 10^{-2} \text{ g} \text{ (g)}$	$M_B = \sum m_i, m_i < 10^{-2} \text{ g} \text{ (g)}$	$M_{\text{scaling}} \text{ (g)}$	$\beta$
Horizontal	$69.0 \pm 0.1$	$68.27 \pm 0.03$	$0.63 \pm 0.01$	0.25	$1.15 \pm 0.05$
Vertical	$57.6 \pm 0.1$	$57.03 \pm 0.03$	$0.48 \pm 0.01$	0.42	$1.17 \pm 0.05$
Vertical	$77.0 \pm 0.1$	$75.59 \pm 0.03$	$1.03 \pm 0.01$	0.74	$1.20 \pm 0.05$

remaining dust and pieces is denoted  $M_B$  and is also given in the table. Obviously, the sum of all the fragments,  $M_A + M_B$ , should equal the original mass,  $M_0$ . Within the uncertainties, this is true for two of the experiments; for the third, 0.3 g is missing.

Assuming a power law with exponent  $\beta$  to be present for all masses down to zero, we have calculated the total mass to be expected,  $M_{\text{scaling}}$ , for pieces smaller than  $10^{-2} \text{ g}$ . This is done by integrating the distribution function times the mass from 0 to  $10^{-2} \text{ g}$ :

$$M_{\text{scaling}} = \int_{0 \text{ g}}^{10^{-2} \text{ g}} n(m) m dm .$$

The results are listed in Table I. As can be seen from the table, the value of  $M_{\text{scaling}}$  are all somewhat less than the experimentally determined  $M_B$ . However, if one calculates which  $\beta$  would correspond to  $M_B$ , the results are  $\beta = 1.20$ , 1.18, and 1.23, respectively. Comparing these values with the observed powers  $\beta = 1.15$ , 1.17, and 1.20 the discrepancies are accounted for by the uncertainties in the exponents ( $\pm 0.05$ ). The conclusion is that the

scaling region need not be confined to the decades measured here, but could very well continue for smaller fragments.

A possible explanation of the observed variations in the values of the exponent  $\beta$  is that  $\beta$  depends on the symmetry of the shock wave and thereby on the morphology of the object being fragmented. By choosing a sample morphology between that of a bar and plate or a plate and cube, it is possible to vary  $\beta$  continuously. For instance, fragmentation of a half cube of dimensions  $55.3 \times 74.2 \times 74.5 \text{ mm}^3$  gave the power  $\beta = 1.48$ . To check for any dependence on the choice of material, experiments were performed on soap, stearic paraffin, and potato. The potato was peeled; the stearic paraffin, soap, and potato were frozen in liquid nitrogen before being fragmented by a hammer. Within the accuracy of the determination of the exponents no significant dependence on material was observed. The dependence of  $\beta$  on morphology for the gypsum objects as well as the results for soap, stearic paraffin, and potato are summarized in Fig. 4. To depict the data on a one-dimensional axis we give a simplified description of the morphology  $d_m = 1 + 2(ab + ac + bc)/(a^2 + b^2 + c^2)$ , where  $a$ ,  $b$ , and  $c$  are the lengths of the three sides. There is a clear correlation between  $\beta$  and  $d_m$ .

In summary, we have observed fragment distributions that obey scaling laws. We suggest that during the short (but finite) time of the fragmentation process the system becomes continuously driven, and that the observed power law is a result of a self-organized critical state [1]. The scaling exponent lies between 1.0 and 1.7, depending on the overall morphology of the object, rather than on the choice of material or on the way in which the object was struck. A bar had the exponent 1.05, a disk 1.08, and a spherical ball 1.63. These findings may be important for understanding the geographical variations in the Gutenberg-Richter law for earthquakes [27,28]. It is possible that the morphology of the Earth's crust (the thickness and width of the geological layer participating in the crack) plays a role in the geographical variation in the scaling exponent [27,28].

P.D. would like to thank the SARC Foundation, Statens Naturvidenskabelige Forskningsråd, Novo's Fond, and the Leon Rosenfeld Fond.

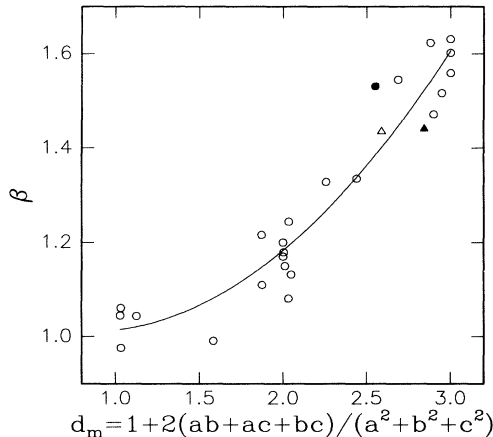


FIG. 4. The values of the scaling exponent  $\beta$  obtained for 26 different objects as a function of a shape parameter  $d_m$ ;  $d_m$  is calculated from the dimensions of the objects  $a$ ,  $b$ , and  $c$ . Data points for gypsum are given as open circles, for soap as a filled circle, for stearic paraffin as a triangle, and for deep frozen potato as a filled triangle. The line is drawn to guide the eye.

\*To whom correspondence should be addressed.

- [1] P. Bak, C. Tang, and K. Wiesenfeld, Phys. Rev. Lett. **59**, 381 (1987).
- [2] P. Bak, C. Tang, and K. Wiesenfeld, Phys. Rev. A **38**, 364 (1988).
- [3] C. Tang and P. Bak, Phys. Rev. Lett. **60**, 2347 (1988).
- [4] B. Gutenberg and C. F. Richter, Seismol. Soc. Am. Bull. **46**, 105 (1956).
- [5] P. Bak and C. Tang, J. Geophys. Res. B **94**, 15635 (1989).
- [6] A. Sornette and D. Sornette, Europhys. Lett. **9**, 197 (1989).
- [7] J. M. Carlson and J. S. Langer, Phys. Rev. Lett. **62**, 2632 (1989).
- [8] J. M. Carlson and J. S. Langer, Phys. Rev. A **40**, 6470 (1989).
- [9] S. S. Manna, Physica (Amsterdam) **179A**, 249 (1991).
- [10] E. N. Miranda and J. H. Herrmann, Physica (Amsterdam) **175A**, 339 (1991).
- [11] Z. Olami, H. J. S. Feder, and K. Christensen, Phys. Rev. Lett. **68**, 1244 (1992).
- [12] K. Christensen, Z. Olami, and P. Bak, Phys. Rev. Lett. **68**, 2417 (1992).
- [13] H. Puhl, Physica (Amsterdam) **182A**, 295 (1992).
- [14] G. A. Held, D. H. Solina, D. T. Keane, W. J. Haag, P. M. Horn, and G. Grinstein, Phys. Rev. Lett. **65**, 1120 (1990).
- [15] S. R. Nagel, Rev. Mod. Phys. **64**, 321 (1992).
- [16] P. Markin, G. Li, L. M. Sander, E. Louis, and F. Guinea, J. Phys. A **22**, 1393 (1989).
- [17] E. Bouchaud, G. Lapasset, and J. Planes, Europhys. Lett. **13**, 73 (1990).
- [18] O. Pla, F. Guinea, E. Louis, G. Li, L. M. Sander, H. Yan, and P. Meakin, Phys. Rev. A **42**, 3670 (1990).
- [19] H. J. Herrman, Phys. Scr. **38**, 13 (1991).
- [20] D. L. Turcotte, J. Geophys. Res. B **91**, 1921 (1986).
- [21] A. Z. Mekjian, Phys. Rev. Lett. **64**, 2125 (1990).
- [22] A. C. Palmer and T. J. O. Sanderson, Proc. R. Soc. London A **433**, 469 (1991).
- [23] T. Ishii and M. Matsushita, J. Phys. Soc. Jpn. **61**, 3474 (1992).
- [24] M. Matsushita and K. Sumida, Bull. Facul. Sci. Eng. **31**, 69 (1988).
- [25] J. J. Gilvarry and B. H. Bergstrom, J. Appl. Phys. **32**, 400 (1961).
- [26] H. E. Stanley and P. Meakin, Nature (London) **335**, 405 (1988).
- [27] M. Matsuzaki, and H. Takayasu, J. Geophys. Res. B **96**, 19925 (1991).
- [28] K. Christensen and Z. Olami, J. Geophys. Res. B **97**, 8729 (1992).